℘

Detection of Elementary Charges on Colloidal Particles

Filip Strubbe, Filip Beunis, and Kristiaan Neyts

Ghent University, Electronics and Information Systems, Sint-Pietersnieuwstraat 41, Ghent B-9000, Belgium
(Received 29 January 2008; published 29 May 2008)

We have succeeded in determining the charge of individual colloidal particles with resolution higher than the elementary charge. The number of elementary charges on a particle is obtained from the analysis of optical tracking data of weakly charged silica spheres in an electric field in a nonpolar medium. The analysis also yields an accurate value of the particle size. Measurement of the charge as a function of time reveals events in which the particle loses or gains an elementary charge due to ionization or recombination processes at the surface.

In recent years, charged colloids with particle charges of just a few to thousands of elementary charges have been studied intensively. Examples are found in soft condensed matter, where colloidal crystals of oppositely charged particles are used as a model for atomic systems [1–3], in biophysics, where enzymatic reactions at the surface of particles are studied by measuring the particle charge [4], in fundamental studies of interparticle interactions [5], and in applications such as electrophoretic displays based on charged pigment particles [6]. For the characterization of charged colloids, measurement techniques are available such as acoustophoresis [7], dynamic and electrophoretic light scattering [8], and phase analysis light scattering [9]. With these methods, average properties of many particles are determined, but no information is obtained on individual particles. Also, due to size and charge polydispersity, the interpretation of the results can be complicated. Recently, optical tracking has been used to measure charges on single particles giving detailed information on individual particles and the distribution of particle charges [10]. However, up to now, the measurement of charges on individual colloidal particles with resolution higher than the elementary charge has not been demonstrated. To some degree, our experiments are comparable with the experiment of Millikan almost 100 years ago [11] in which the elementary charge was determined by using liquid drops in an electric field in air. This method has been optimized and is now used in the search for fractional charges [12]. Finding the elementary charge in a liquid is much harder, because of the higher viscosity, which reduces the motion of weakly charged particles in an electric field to a value which may be below the sensitivity of most measurement systems or difficult to separate from Brownian motion. In this work, we use optical tracking electrophoresis and analysis of multiple mobility measurements to obtain the number of elementary charges on colloidal particles carrying only a few elementary charges in a nonpolar medium. We demonstrate that our method allows monitoring of single ionic reactions at the particle surface and precise measurement of the particle charge and size. This approach

opens possibilities for the characterization of colloidal particles, the (dynamic) study of charging mechanisms, the monitoring of chemical or electrochemical reactions, and the detection of (bio)molecules bound to particles.

In our study, we use spherical silica particles (Mo-Sci) with radius 1.05 ± 0.05 μm in the nonpolar solvent dodecane (Rectapur, VWR) at volume fractions below 0.01. Because of the low dielectric constant ($\varepsilon = 2$) and the large Bjerrum length (28 nm) of dodecane, individual charges are very rare [13]. As a result. also the charge of the silica particles in dodecane is low: For 120 particles, the charge determined by standard electrophoretic measurement [14] was in the range between $-70e$ and $+20e$, with e the elementary charge. This is more than 100 times smaller than in water ($\varepsilon = 80$) [15]. Because of the low charge concentration, electro-osmosis can be neglected.

We use a standard optical electrophoresis setup [16] to track individual particles while they are moving in an electric field generated by applying a square wave voltage. The optical system consists of an optical microscope and a CCD camera, with a total optical magnification of 169.5 nm per pixel on the CCD camera. A square wave voltage of amplitude $V = 100$ V and frequency 2 Hz is applied over the electrodes. Since parallel electrodes are used, the amplitude of the electrical field E is simply $E = V/d$, where the distance d is determined by measuring the number of pixels between the electrodes, a typical value being 80 μm. The amplitude of the electrical field is therefore about 10^6 V/m. Images are taken at 20 Hz, and image analysis based on the particle centroid results in an accuracy of about 20 nm. During each half period of the square wave voltage, the electrophoretic mobility μ of a particle is determined as its speed along the direction of the field ($\Delta x/\Delta t$ based on two samples with $\Delta t = 0.15$ s) divided by the amplitude of the electrical field. The particle position along the field as a function of time has roughly a triangular shape [Fig. 1(a)]. The position perpendicular to the field is governed by Brownian motion. Typically, 120 values of the electrophoretic mobility are calculated for each particle over a period of 30 seconds [Fig. 1(b)].
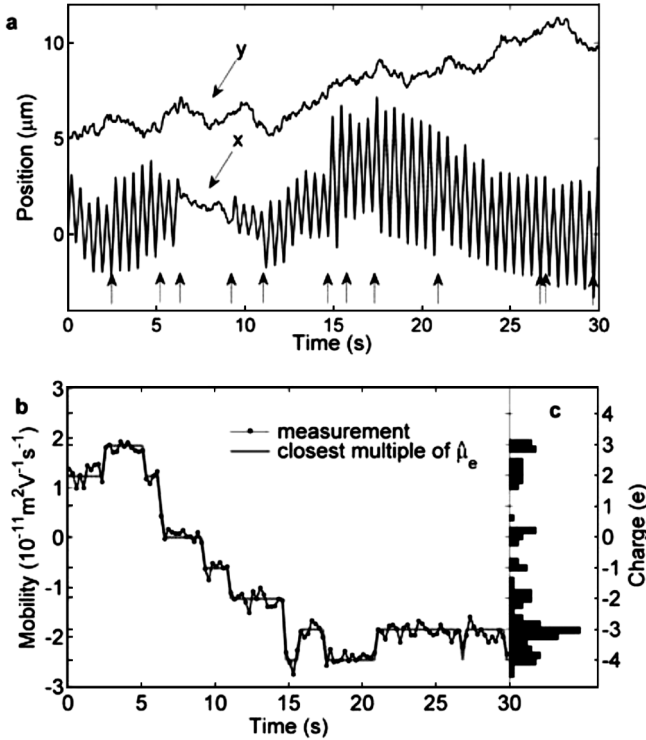
FIG. 1. Electrophoretic measurement of a silica particle in dodecane. (a) The particle position (x, relative to the initial position) during the application of a square wave voltage, resulting in a typical triangular shape with changing amplitude as the particle charge changes (indicated by arrows). The Brownian motion in the y direction perpendicular to the field (with chosen initial position 5 μm) is unaffected by the field. (b) The 120 corresponding mobilities are shown, and guidelines indicate multiples of the elementary mobility $\hat{\mu}_e$. (c) Histogram of the electrophoretic mobility showing peaks at multiples of the elementary mobility. The right axis indicates the number of elementary charges.

We will now verify that elementary charges are resolved. The electrical charge Z (in units of e) of a spherical particle in the absence of an electrolyte can be calculated from the electrophoretic mobility with the Stokes-Einstein relation:

$$\mu = Ze/6\pi\eta a, \qquad (1)$$

with a the hydrodynamic radius of the particle and η the viscosity of the solvent. The Debye length in our silica suspensions is larger than 10 μm, so the Hückel limit can be used for 1 μm particles [17]. From the known radius $a = 1.05$ μm and $\eta = 1.38 \times 10^{-3}$ Pa s, we obtain $\mu \approx 6 \times 10^{-12}$ m^2 V^{-1} s^{-1} for a particle carrying a unit charge. This value agrees well with the distance between the peaks in the experimental histogram of the electrophoretic mobility [Fig. 1(c)]. The peaks in the mobility histogram indicate that the particle charge Z varies in discrete steps and confirm that the elementary charge is resolved.

There are two disadvantages of using Eq. (1) to calculate the particle charge. First, the particle size is in many cases

not accurately known (in our case, only the average size is provided by the manufacturer). Second, the accuracy of a mobility measurement is limited by inherent Brownian motion. The standard deviation (σ_μ) for the measured electrophoretic mobility values can be estimated as:

$$\sigma_\mu = \frac{1}{E}\sqrt{\frac{2D}{\Delta t}}, \qquad (2)$$

which is the ratio of the mean displacement in one dimension due to Brownian motion $\sqrt{2D\Delta t}$ [16] over the field-induced motion $\mu E \Delta t$, multiplied with μ. Here D represents the self-diffusion constant of the particle.

We will now show how a detailed analysis of multiple mobility measurements can yield highly accurate values of the particle size and the particle charge as a function of time, without using Eq. (1), but by taking advantage of the discrete nature of the electric charge and the known value of the unit charge. In a typical experiment, M mobilities μ_i (with $i = 1, \ldots, M$) are measured on a single spherical particle of unknown radius a that can be modeled as

$$\mu_i = Z_i\mu_e + \varepsilon_i. \qquad (3)$$

Here Z_i are integers representing the discrete charge in units of e, μ_e is the elementary mobility of a particle with radius a and charge e, and ε_i is the error on the measurement. We assume that the error ε_i due to Brownian motion or measurement limitations is uncorrelated and normally distributed, with average 0 and variance σ^2. We want to find estimations for the elementary mobility $\hat{\mu}_e$, the number of charges $\hat{Z}_i$, the variance $\hat{\sigma}^2$, the particle size $\hat{a}$, and the diffusion constant $\hat{D}$ (with ˆ referring to estimated values). If σ is small compared to μ_e, the values μ_i will be clustered around multiples of the elementary mobility μ_e as illustrated in Fig. 1(c). If the condition $\varepsilon_i \ll \mu_e$ is fulfilled, we find with Eq. (3) that $Z_i \cong \mu_i/\mu_e$ and, since Z_i is an integer, that $Z_i = [\mu_i/\mu_e]$, where the brackets mean rounding to the nearest integer. We can then rewrite Eq. (3):

$$\mu_i - [\mu_i/\mu_e]\mu_e = \varepsilon_i \ll \mu_e. \qquad (4)$$

Now we evaluate the function $R^2(\mu)$, which is the sum of squares of the residuals ε_i from Eq. (4) where we replace the unknown value of μ_e by μ:

$$R^2(\mu) = \sum_{i=1}^{M}(\mu_i - [\mu_i/\mu]\mu)^2. \qquad (5)$$

For completely random mobility data, the sum of squares in Eq. (5) has an expectancy $M\mu^2/12$. If the mobility data are clustered around multiples of μ_e, we expect $R^2(\mu)$ to be significantly smaller than $M\mu^2/12$ for the value of μ_e. Therefore, the elementary mobility $\hat{\mu}_e$ should correspond to a local minimum in $R^2(\mu)$. In practice, we determine searching intervals satisfying $R^2(\mu) \leq 0.7 \times M\mu^2/12$ and calculate the lowest local minimum. Another method
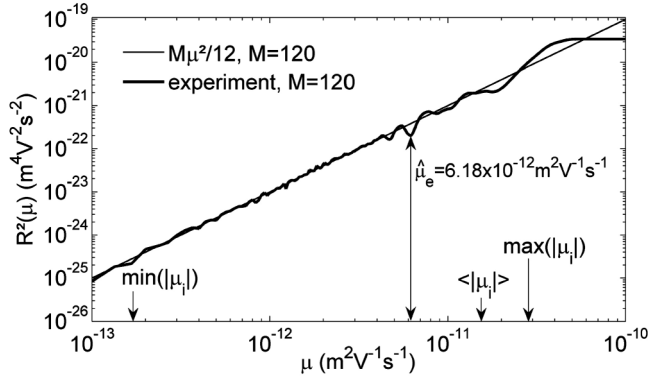
FIG. 2. Analysis of the electrophoretic mobilities from Fig. 1(b). $R^2(\mu)$ from Eq. (5) is shown for the experiment in Fig. 1, with $M = 120$. The straight line shows the quadratic expectancy $M\mu^2/12$ for random mobility data and $M = 120$. Values of the experimental curve that are below this quadratic trend indicate a clustering around multiples of the corresponding mobility μ. $\hat{\mu}_e$ is determined as the local minimum indicated by the double arrow. The minimum, maximum, and average of the absolute value of the measured mobilities are also indicated.

FIG. 3. High resolution charge histogram. The 1200 measurements on 10 particles of the charge $\tilde{Z}_i = \mu_i/\hat{\mu}_e$ show peaks in the charge histogram at multiples of the elementary charge e.

would be to determine an approximate value of μ_e, for instance, by analyzing the Brownian motion in the y direction, and to locate the closest local minimum. Figure 2 shows $R^2(\mu)$ using the mobilities from Fig. 1(b) with $M = 120$. For this experiment, we find $\hat{\mu}_e = 6.18 \times 10^{-12}$ m^2 V^{-1} s^{-1}, and the corresponding error is about 0.05×10^{-12} m^2 V^{-1} s^{-1} (see below). The detailed shape of $R^2(\mu)$ depends on the values of Z_i that have occurred during the experiment. For values of μ higher than $2 \times$ max($|\mu_i|$), $R^2(\mu)$ becomes constant as expected.

Once $\hat{\mu}_e$ is known, accurate estimations can be made of the particle radius $\hat{a} = e/6\pi\eta\hat{\mu}_e$ and the diffusion constant $\hat{D} = \hat{\mu}_e kT/e$ using the Stokes and Einstein relations, with k the Boltzmann constant and T the absolute temperature. Each measured mobility μ_i corresponds to an estimation of the number of elementary charges $\tilde{Z}_i = \mu_i/\hat{\mu}_e$, which is, in general, not an integer, due to the measurement error in μ_i. Since the charge is a multiple of the elementary charge, we find the most probable value of Z by rounding to the nearest integer: $\hat{Z}_i = [\mu_i/\hat{\mu}_e]$. For particles with a given standard deviation of the mobility σ, the fraction of correctly estimated values $\hat{Z}_i = Z_i$ is given by erf($\mu_e/\sqrt{8}\sigma$). In our experiments, this fraction is typically 98% (for 2% of the estimations, the error is one unit: $\hat{Z}_i = Z_i \pm 1$). The variance of the error ε_i is calculated as $\hat{\sigma}^2 = \sum(\mu_i - \hat{Z}_i\hat{\mu}_e)^2/(M - 1)$ and is related to the sum of squares of the residual mobility in (5) by $\hat{\sigma}^2 = R^2(\hat{\mu}_e)/(M - 1)$.

The histogram in Fig. 3 is obtained by using the 1200 values of $\tilde{Z}_i = \mu_i/\hat{\mu}_e$ for 10 particles, where $\hat{\mu}_e$ is the value determined for the corresponding particle. It illustrates the clustering of data around whole numbers, but, because of the limited number of particles, it does not

represent the true particle charge probability distribution. The charge on the silica particles is between $-12e$ and $+10e$, and there is about one exchange ($\pm e$) per second with a decrease ($-e$) being slightly more frequent (58%) than an increase (42%). Such fluctuations cannot be observed with conventional methods that average over large numbers of particles and/or longer time intervals. The principle charging mechanism for silica particles in water is dissociation of silanol groups [15]: SiOH$\rightleftharpoons$SiO$^-$ + H$^+$. In nonaqueous media such as dodecane, the charging mechanism of silica particles is not fully understood [13]. Probably the mechanism is similar, but charging events are less frequent in nonpolar media due to the stronger electrostatic interaction between charges.

Analysis of the error on $\hat{\mu}_e$ and the calculated properties that are derived from it is quite complicated and depends on the values Z_i and σ/μ_e. In the theoretical limit $\sigma/\mu_e \ll 1$, the overlap between the peaks in the mobility histogram is negligible, and the charge is always estimated correctly: $\hat{Z}_i = Z_i$. In this case, the variance $\sigma_{\hat{\mu}_e}^2$ of $\hat{\mu}_e$ can simply be obtained by using the (Z_i, μ_i) data and applying standard linear regression theory:

$$\sigma_{\hat{\mu}_e}^2 = \sigma^2 \Big/ \sum_i Z_i^2. \qquad (6)$$

In our experiments, the typical value of σ/μ_e is 0.21, which is not negligible compared to 1, so we expect the variance to be larger than the formula given in (6). We estimate the variance on $\hat{\mu}_e$ (denoted $\hat{\sigma}_{\hat{\mu}_e}^2$) by constructing 100 sets of randomly generated mobility data (also containing 120 values per series) according to the normal distribution $N(\hat{Z}_i\hat{\mu}_e, \hat{\sigma}^2)$, by using the values of $\hat{\mu}_e$, $\hat{Z}_i$, and $\hat{\sigma}$ calculated from the experiment. Then we use the described algorithm to calculate $R^2(\mu)$ and estimate the elementary mobility for each of the 100 data sets. The standard deviation of the 100 values of the elementary mobility obtained in this way is defined as $\hat{\sigma}_{\hat{\mu}_e}$ and is in our experiments typically 20% higher than Eq. (6). Typical

TABLE I. Measurement results for 3 silica particles in dodecane. The results for particle 1 are obtained from the data in Figs. 1 and 2. The values of $\hat{\mu}_e$, $\hat{\sigma}_{\hat{\mu}_e}$, $\hat{\sigma}$, and σ_μ in the table have to be multiplied by 10^{-12} m^2 V^{-1} s^{-1}.

$\hat{\mu}_e \pm \hat{\sigma}_{\hat{\mu}_e}$	$\hat{a}$ (μm)	$\hat{\sigma}$	σ_μ	$\sqrt{(1/M)\sum_i \hat{Z}_i^2}$
6.18 ± 0.05	0.996 ± 0.008	1.30	1.32	2.76
6.10 ± 0.01	1.009 ± 0.002	1.16	1.25	8.43
5.97 ± 0.02	1.032 ± 0.003	1.24	1.17	9.08

values for $\hat{\sigma}_{\hat{\mu}_e}/\hat{\mu}_e$ in our experiments are between 0.2% and 2%.

We have listed the resulting properties $\hat{\mu}_e$, $\hat{\sigma}_{\hat{\mu}_e}$, $\hat{a}$, $\hat{\sigma}$, σ_μ, and $\sqrt{(1/M)\sum_{i=1}^{M} \hat{Z}_i^2}$ for 3 particles in Table I, each determined from $M = 120$ mobility measurements. The resulting particle sizes are in the range specified by the manufacturer. The accuracy of the particle size measurement of a few nanometers is sufficient to reveal small variations in the sizes of the particles. Notice that the accuracy of the elementary mobility measurement ($\hat{\sigma}_{\hat{\mu}_e} \approx 5 \times 10^{-14}$ m^2 V^{-1} s^{-1}) is about 30 times higher than the accuracy of a single mobility measurement ($\hat{\sigma} \approx 1.3 \times 10^{-12}$ m^2 V^{-1} s^{-1}). The accuracy is higher if the value of $\sqrt{(1/M)\sum_{i=1}^{M} \hat{Z}_i^2}$ is larger, which can be understood from Eq. (6). The values $\hat{\sigma}$ and σ_μ are approximately the same, indicating that Brownian motion is the main source of error. Because we use monodisperse particles with known average size $a = 1.05$ μm, we can combine a with $\hat{\mu}_e$ to estimate the elementary charge: $\hat{e} = 6\pi\eta a\hat{\mu}_e$. The value for the elementary charge for 10 particles $\hat{e} = (1.64 \pm 0.05) \times 10^{-19}$ C corresponds with the well known value for e.

The accuracy of the method can be optimized by increasing the number of measurements per particle and by minimizing the error of a single mobility measurement as can be seen from Eq. (6). Since Brownian motion is the main error contribution to the mobility measurement, the latter can be achieved by making σ_μ small compared to μ_e. As can be seen from Eq. (2), this can be achieved by increasing the electric field (while avoiding electrochemical reactions) and the measurement time (not above the

typical time for charge exchange) and by using small particles. In polar media, the detection of single charges may be more difficult and require smaller particles, higher frequencies, and/or faster detection.

In conclusion, we have demonstrated that the number of elementary charges on a particle, the particle size, and the occurrence of single ionic reactions at the surface can be measured for weakly charged particles in a nonpolar liquid. This method can be used for characterizing weakly charged colloids—especially in nonpolar media—and for studying fundamental electrokinetic phenomena. This method may find useful applications in colloid chemistry and single molecule biology, where the binding of single biomolecules on the particle surface can be detected [18].

[1] M. E. Leunissen *et al.*, Nature (London) **437**, 235 (2005).
[2] E. V. Shevchenko *et al.*, Nature (London) **439**, 55 (2006).
[3] P. Bartlett and A. I. Campbell, Phys. Rev. Lett. **95**, 128302 (2005).
[4] R. Galneder *et al.*, Biophys. J. **80**, 2298 (2001).
[5] M. F. Hsu, E. R. Dufresne and D. A. Weitz, Langmuir **21**, 4881 (2005).
[6] B. Comiskey *et al.*, Nature (London) **394**, 253 (1998).
[7] S. Durand-Vidal *et al.*, Colloids Surf. A **267**, 117 (2005).
[8] J. Y. Lee *et al.*, J. Nanosci. Nanotechnol. **5**, 1045 (2005).
[9] J. F. Miller, K. Schätzel, and B. Vincent, J. Colloid Interface Sci. **143**, 532 (1991).
[10] G. S. Roberts *et al.*, J. Chem. Phys. **126**, 194503 (2007).
[11] R. A. Millikan, Phys. Rev. **32**, 349 (1911).
[12] V. Halyo *et al.*, Phys. Rev. Lett. **84**, 2576 (2000).
[13] I. D. Morrison, Colloids Surf. A **71**, 1 (1993).
[14] F. Strubbe, F. Beunis, and K. Neyts, J. Colloid Interface Sci. **301**, 302 (2006).
[15] S. H. Behrens and D. G. Grier, J. Chem. Phys. **115**, 6716 (2001).
[16] J. C. Crocker and D. G. Grier, J. Colloid Interface Sci. **179**, 298 (1996).
[17] A. V. Delgado *et al.*, Pure Appl. Chem. **77**, 1753 (2005).
[18] A. M. Armani *et al.*, Science **317**, 783 (2007).